

Single photoionization of the Kr-like Rb II ion in the photon energy range 22 - 46.0 eV

Brendan M. McLaughlin^{1,2*} and James F. Babb^{2†}

¹Centre for Theoretical Atomic and Molecular Physics (CTAMOP), School of Mathematics and Physics, Queen's University Belfast, Belfast BT7 1NN, UK

²Institute for Theoretical Atomic and Molecular Physics (ITAMP), Harvard Smithsonian Center for Astrophysics, MS-14, Cambridge, MA 02138, USA

Draft: 12 April 2019

ABSTRACT

Single photoionization cross sections for Kr-like Rb⁺ ions are reported in the energy (wavelength) range 22 eV (564 Å) to 46 eV (270 Å). Theoretical cross section calculations for this *trans*-Fe element are compared with measurements from the ASTRID radiation facility in Aarhus, Denmark and the dual laser plasma (DLP) technique, at respectively 40 meV and 35 meV FWHM energy resolution. In the photon energy region 22 - 32 eV the spectrum is dominated by excitation autoionizing resonance states. Above 32 eV the cross section exhibit classic Fano window resonances features, which are analysed and discussed. Large-scale theoretical photoionization cross-section calculations, performed using a Dirac Coulomb *R*-matrix approximation are bench marked against these high resolution experimental results. Comparison of the theoretical work with the experimental studies allowed the identification of resonance features and their parameters in the spectra in addition to contributions from excited metastable states of the Rb⁺ ions.

Key words: atomic data – atomic processes – scattering

1 INTRODUCTION

Rb I optical pumping lines have been observed in AGB stars, and both isotopes of Rb I (⁸⁵Rb I and ⁸⁷Rb I) are present based on the presence of s-process elements such as Zr (Darling 2018). A major source of discrepancy is the quality of the atomic data used in the modelling (Snedden et al. 1991; Mishenina et al. 2002; Roederer et al. 2011, 2010; Frebel et al. 2014).

The motivation for the current study of this *trans*-Fe element, Rb II, is to provide benchmark PI cross section data for applications in astrophysics. High-resolution measurements of the photoionization cross section of Rb⁺ were recently performed at the ALS synchrotron radiation facility in Berkeley, California (Mueller et al. 2013), over the photon energy range 22 – 46 eV at a resolution of 18 meV FWHM. Many excited Rydberg states have been identified in the energy (wavelength) range 22 eV (564 Å) to 46 eV (270 Å). Large-scale DARC PI cross section calculations when compared with previous synchrotron radiation (SR) and dual laser plasma (DLP) experimental studies (Kilbane et al.

2007) indicate excellent agreement. Such comparisons give confidence in our theoretical data for use in astrophysical applications.

To the authors knowledge, we are aware only of experimental and theoretical work on PI for this *trans*-Fe element, Rb II, performed recently at the Advanced Light Source (ALS) (Mueller et al. 2013), the joint study by Kilbane et al. (2007), using a merged-beams technique by combining synchrotron radiation (SR) with a beam of Rb⁺ (Rb II) ions at the ASTRID synchrotron radiation facility, the dual laser plasma (DLP) technique, at Dublin City University (DCU), and the theoretical study of Demekhin et al. (2007). This updated earlier work carried out using the DLP technique by Neogi et al. (2003).

2 THEORY

2.1 Atomic Structure

The GRASP code (Dyall et al. 1989; Parpia et al. 2006; Grant 2007) generated the target wave functions employed in the present work. All orbitals were physical up to $n=3$, $4s$, $4p$ and $4d$. We initially used an extended averaged level (EAL) calculation for the $n = 3$ orbitals. The EAL calculations

* E-mail:bmclaughlin899@btinternet.com

† E-mail:jbabb@cfa.harvard.edu

Table 1. Rb^{2+} energy levels in Rydbergs (Ry) from the large-scale GRASP calculations compared with the available tabulations from the NIST database (Kramida et al. 2018). A sample of the lowest 13 levels for the residual Rb^{2+} ion from the 456-level GRASP calculations are shown compared to experiment. The percentage difference $\Delta(\%)$ compared to experiment of individual energy levels is given for completeness.

Level	STATE	TERM	NIST (Ry)	GRASP (Ry)	$\Delta(\%)^a$
1	$4s^2 4p^5$	$2P_{3/2}^o$	0.00000	0.00000	0.0
2	$4s^2 4p^5$	$2P_{1/2}^o$	0.06720	0.06678	0.6
3	$4s 4p^6$	$2S_{1/2}$	1.18494	1.22287	3.2
4	$4s^2 4p^4 ({}^3P) 4d$	$4D_{7/2}$	1.40992	1.44446	2.5
5	$4s^2 4p^4 ({}^3P) 4d$	$4D_{5/2}$	1.41135	1.44680	2.5
6	$4s^2 4p^4 ({}^3P) 4d$	$4D_{3/2}$	1.41761	1.45368	2.5
7	$4s^2 4p^4 ({}^3P) 4d$	$4D_{1/2}$	1.42516	1.46140	2.5
8	$4s^2 4p^4 ({}^3P) 4d$	$4F_{9/2}$	1.48462	1.53650	3.5
9	$4s^2 4p^4 ({}^3P) 4d$	$4F_{7/2}$	1.50853	1.56335	3.6
10	$4s^2 4p^4 ({}^3P) 4d$	$4F_{5/2}$	1.52929	1.58192	3.4
11	$4s^2 4p^4 ({}^3P) 4d$	$4F_{3/2}$	1.53777	1.59050	3.4
12	$4s^2 4p^4 ({}^1P) 4d$	$2P_{1/2}$	1.51351	1.59218	5.2
13	$4s^2 4p^4 ({}^1P) 4d$	$2D_{3/2}$	1.56776	1.62083	3.4

^a Absolute percentage difference, $\Delta(\%)$, between theoretical and experimental energy levels for the Rb III ion. The average $\Delta(\%)$ of the energy levels with experiment is $\approx 3\%$.

were performed on the lowest 13 fine-structure levels of the residual Rb III ion. In our work we retained all the 456 - levels originating from one, two and three-electron promotions from the $n=4$ levels into the orbital space of this ion. All 456 levels arising from the six configurations were included in the DARC close-coupling calculation, namely: $3s^2 3p^6 3d^{10} 4s^2 4p^5$, $3s^2 3p^6 3d^{10} 4s 4p^6$, $3s^2 3p^6 3d^{10} 4s^2 4p^4 4d$, $3s^2 3p^6 3d^{10} 4s 4p^5 4d$, $3s^2 3p^6 3d^{10} 4s^2 4p^3 4d^2$, and $3s^2 3p^6 3d^{10} 4s^2 4p^2 4d^3$.

Table 1 shows the theoretical energy levels from the 456-level GRASP calculations for the lowest 13 levels of the residual Rb^{2+} ion, compared to the values available from the NIST tabulations (Kramida et al. 2018). The average percentage difference of our theoretical energy levels compared with the NIST values is approximately 3% higher.

Photoionization cross sections calculations were carried out on the Rb II ion for the $3d^{10} 4s^2 4p^6 \ ^1S_0$ ground state, $3d^9 4s^2 4p^5 5s \ ^3P_{2,1,0}$, $3d^9 4s^2 4p^5 5s \ ^1P_1$ and the $3d^9 4s^2 4p^5 4d \ ^3P_{2,1,0}$ metastable levels using the DARC codes.

2.2 Photoionization calculations

The scattering calculations were performed for photoionization cross sections using the above large-scale configuration interaction (CI) target wavefunctions as input to the parallel DARC suite of R -matrix codes. The latest examples of the DARC R -matrix method, implemented in our parallel suite of codes to predict accurate photoionization cross sections are the recent experimental and theoretical studies on the Zn II trans - Fe ion by Hinojosa et al. (2017) and the Ca II ion by Müller et al. (2017).

Table 2. Resonance energies E_n of the $4s^2 4p^5 ({}^2P_{1/2}^o) ns \ ^1P_1^o$ Rydberg series from the present 456-level DARC calculations, converging to the $\text{Rb}^{2+} (3d^{10} 4s^2 4p^5 \ ^2P_{1/2}^o)$ threshold, originating from the $\text{Rb}^+ (3d^{10} 4s^2 4p^6 \ ^1S_0)$ ground state. The quantum defect μ for the Rydberg series and linewidths Γ (μeV) are included for completeness. This series is not detectable in the experimental studies due to the extremely narrow resonance linewidths.

Label ns	Theory E_n (eV)	Theory μ_n	Theory Γ (μeV)
8s	–	–	–
9s	27.4233	0.6502	214
10s	27.5815	0.6493	151
11s	27.6960	0.6487	110
12s	27.7816	0.6482	83
13s	27.8472	0.6479	64
14s	27.8986	0.6476	51
15s	27.9397	0.6474	41
16s	27.9730	0.6474	33
⋮			
Limit	28.204	–	–

Sixteen continuum orbitals were used in our scattering calculations. A boundary radius of 9.82 a_0 was necessary to accommodate the diffuse $n = 4$ bound state orbitals of the residual Rb III ion. To resolve all the fine resonance features in the spectra, we used an energy grid of $2 \times 10^{-7} \mathcal{Z}^2 Ry$ (13.6 μeV), where $\mathcal{Z} = 2$, in our calculations.

Photoionization cross section calculations with this 456-level model were carried out using the above energy mesh for the $3d^{10} 4s^2 4p^6 \ ^1S_0$ ground state the $3d^9 4s^2 4p^5 5s \ ^3P_{2,1,0}$, $3d^9 4s^2 4p^5 5s \ ^1P_{1,0}$, and $3d^9 4s^2 4p^5 4d \ ^3P_{2,1,0}$ metastable levels of this ion, over the photon energy range similar to experimental studies.

For the 1S_0 ground state level we require only the bound-free dipole matrices, $J^\pi = 0^e, \rightarrow J'^{\pi'} = 1^o$. In the case of the metastable levels we required the following, $J^\pi = 2^o, \rightarrow J'^{\pi'} = 1^e, 2^e, 3^e$, for $J^\pi = 1^o, \rightarrow J'^{\pi'} = 0^e, 1^e, 2^e$ and $J^\pi = 0^o, \rightarrow J'^{\pi'} = 1^e$, bound-free dipole matrices. The Hamiltonian diagonal matrices were shifted to the recommended experimental NIST tabulated (Kramida et al. 2018) values. Such an energy adjustment provides better positioning of resonances energies relative to all thresholds.

2.3 Resonances

The NIST tabulations (Kramida et al. 2018) for the Rb II energy levels were a helpful guidance for the present resonance assignments. The time-delay of the S -matrix method (Smith 1960), applicable to atomic and molecular complexes, for locating narrow resonances, as developed by Berrington and co-workers (Quigley & Berrington 1996; Quigley et al. 1998; Ballance et al. 1999) was used to locate and determine the resonance positions. This procedure was used in our recent study on the trans-Fe element Zn II (Hinojosa et al. 2017) to locate all the resonances in the spectra.

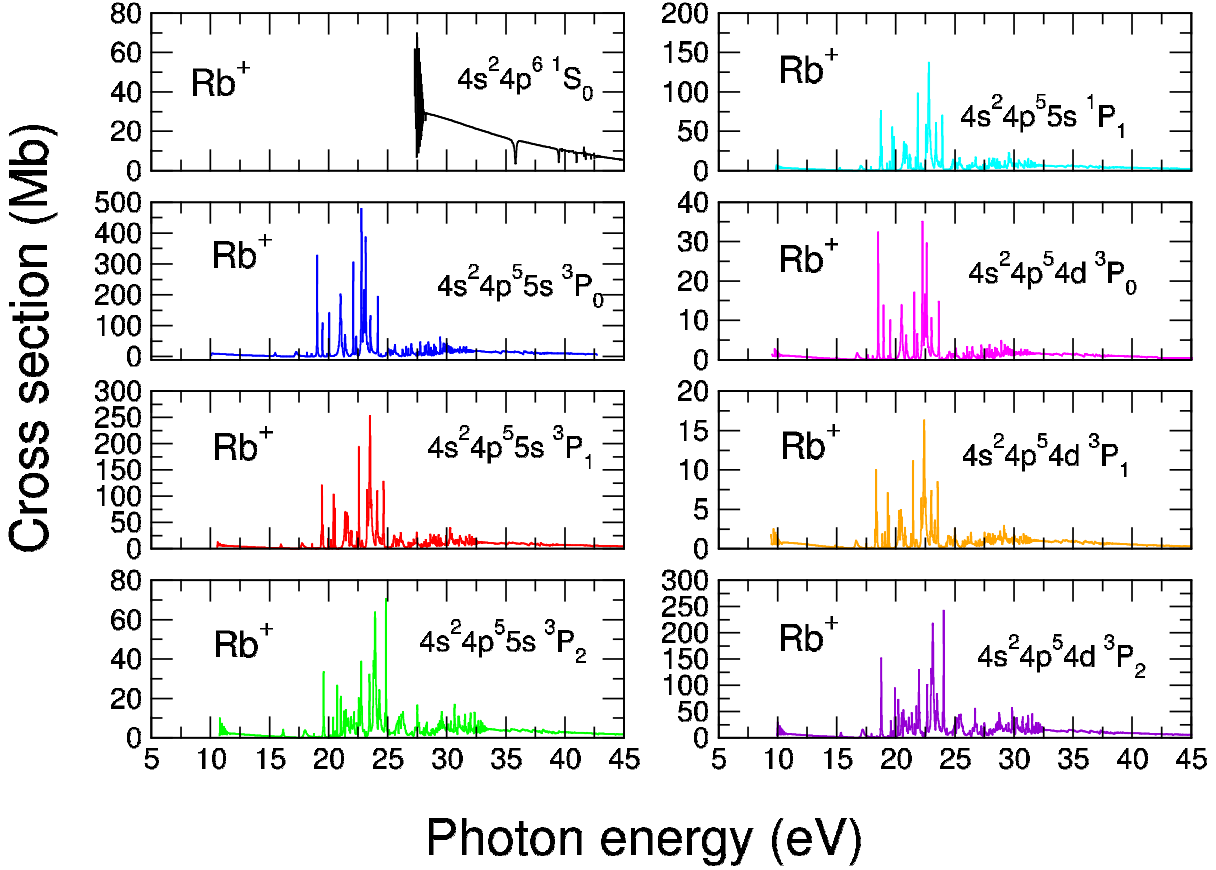


Figure 1. (Colour online) Single photoionization cross sections for Rb^+ ions in the photon energy region 5 – 45 eV. Results are illustrated for the 456-level Dirac R -matrix approximation, for photon energies from threshold to 45 eV, for the $4s^2 4p^6 \ ^1S_0$ ground state, the $4s^2 4p^5 5s \ ^3P_{2,1,0}$, $4s^2 4p^5 5s \ ^1P_1$, and the $4s^2 4p^5 4d \ ^3P_{0,1,2}$ metastable levels. The theoretical cross sections from the 456-level DARC calculations were convoluted with a Gaussian distribution having a profile width of 18 meV.

3 RESULTS AND DISCUSSION

The 456-level DARC PI calculations are shown in Figure 1. to illustrate the single photoionization cross sections contributions from both the ground and the metastable states in the region from threshold to 45 eV, for the Rb^+ ions in their $4s^2 4p^6 \ ^1S_0$ ground state, the $4s^2 4p^5 5s \ ^3P_{2,1,0}$, $4s^2 4p^5 5s \ ^1P_1$ and the $4s^2 4p^5 4d \ ^3P_{0,1,2}$ metastable states. We statistically averaged the contribution from the metastable levels and then use a best fit with the experimental measurements to identify the metastable content in the beam.

In Figure 2 we illustrate our DARC 456-level calculations over the photon energy range 22 – 46 eV. We make the assumption that 98% of the $4s^2 4p^6 \ ^1S_0$ ground state and 2% of the statistically averaged excited metastable states : $4s^2 4p^5 5s \ ^3P_{2,1,0}$, $4s^2 4p^5 5s \ ^1P_1$ and $4s^2 4p^5 4d \ ^3P_{0,1,2}$ will give the best match with the ALS experimental data taken at 18 meV FWHM (Mueller et al. 2013).

Prior dual laser plasma (DLP) measurements at Dublin City University (DCU) made at 35 meV and synchrotron

measurements performed on ASTRID at 40 meV (Kilbane et al. 2007) are compared with our DARC calculations. These comparisons are illustrated in figure 3 and figure 4 respectively. Figure 3 shows the comparison of our present DARC calculations with the DLP measurements taken at 35 meV FWHM in the photon energy region 27 - 28.6 where excellent agreement between theory and experiment is seen. In figure 4, a comparison with our present DARC PI calculations and the measurements from the ASTRID radiation facility in Aarhus (taken at a photon resolution of 40 meV) is made in the photon region where the prominent Fano window resonances are located. Here again excellent agreement between theory and experiment is observed. The good agreement with the available experimental measurements provides further confidence in our theoretical cross section data for astrophysical applications.

From these investigations we see that the PI cross sections below 32 eV are dominated by strong Feshbach resonances, while above 32 eV there are strong dips in the PI

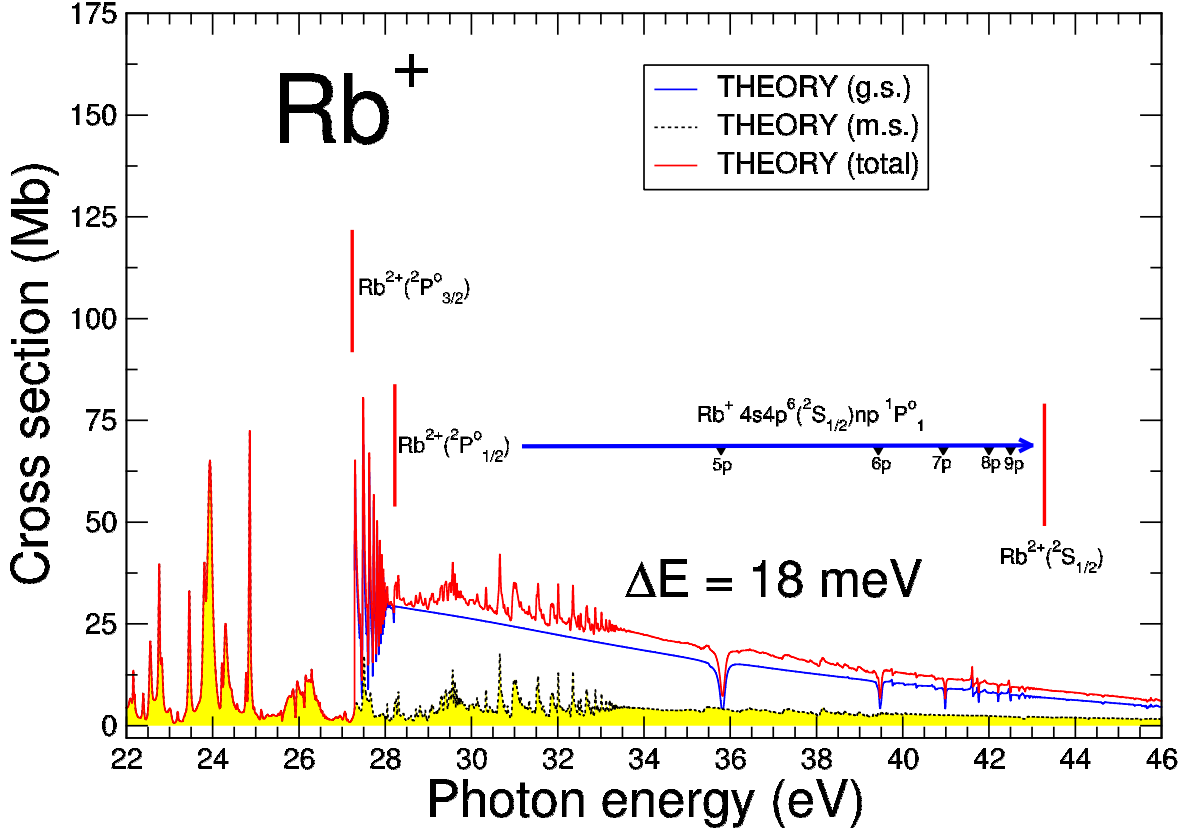


Figure 2. (Colour online) Single photoionization cross section of Rb^+ : DARC 456-level theoretical results. The theoretical data were convoluted with a Gaussian distribution having a profile width of 18 meV and an appropriate admixture used (see text for details) for the ground state and the metastable states. The Fano window resonances $4s4p^6(^2S_{1/2})np\ ^1P^{\circ}_1$ (inverted black triangles) are shown in the photon energy region 34 eV – 43 eV.

cross section due to Fano window style resonances. In the energy range from the ground state threshold to 28 eV, Feshbach $\text{Rb}^+(3d^{10}4s^24p^5ns, md\ ^1S_0)$ dominate the cross section. The Fano Rydberg window resonance series originates from photo-excitation of the inner shell 4s-electron to the outer np orbital, $n \geq 5$, when the $\text{Rb}^+(3d^{10}4s^24p^6\ ^1S_0)$ ion is in its ground state. The narrow Feshbach $4s^24p^5ns$ resonances (~ 0.2 meV or less), which are tabulated in Table 2, are not detectable in the experimental studies due to the limited experimental resolution, at best 18 meV, from the ALS work. The results for the broader $4s^24p^5nd$ are presented in Table 3, where they are compared with previous experimental studies (Neogi et al. 2003; Kilbane et al. 2007). Finally, in Table 4, the first few members of the Fano window resonances, $4s \rightarrow np$, $n \geq 5$, are tabulated and their values compared with the previous dual laser plasma (DLP) and those from the ASTRID synchrotron radiation (SR) facility experimental studies (Neogi et al. 2003; Kilbane et al. 2007).

The theoretical integrated continuum oscillator strength f may also be compared with experiment when available. The integrated continuum oscillator strength f of the experimental spectra may be calculated over the energy grid $[E_1, E_2]$, where E_1 is the minimum experimental energy and E_2 is the maximum experimental energy measured, using (Shore 1967; Fano & Cooper 1968; Berkowitz 1979),

$$\begin{aligned} f &= 9.1075 \times 10^{-3} \int_{E_1}^{E_2} \sigma(h\nu) d h\nu \\ &= 9.1075 \times 10^{-3} \bar{\sigma}_{\text{PI}} \end{aligned}$$

where

$$\bar{\sigma}_{\text{PI}} = \int_{E_1}^{E_2} \sigma(h\nu) d h\nu \quad (1)$$

is the resonance strength. Evaluating the continuum oscillator strength from the DARC theoretical R -matrix cross sections gave a value of 3.60 for 98% of the $4s^24p^6\ ^1S_0$

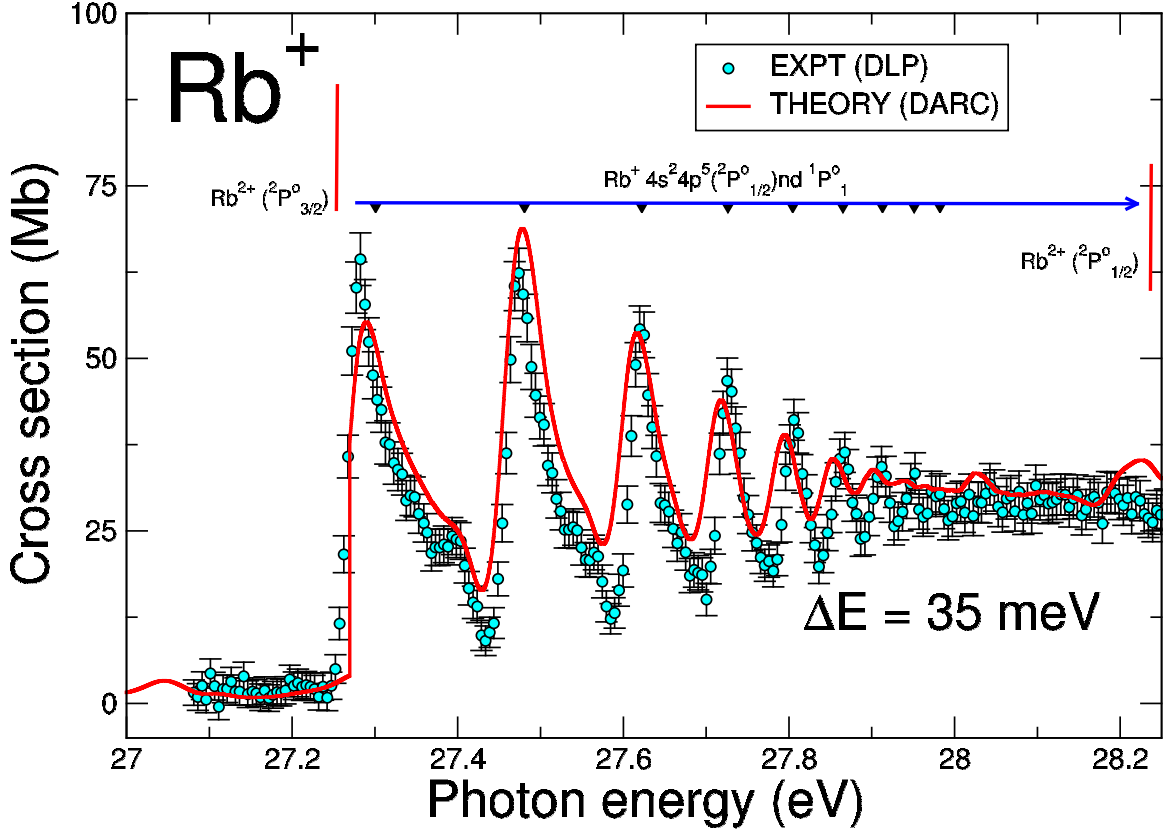


Figure 3. (Colour online) Single photoionization cross section of Rb^+ in the photon energy region 27 - 28.25 eV. Experimental measurements (solid cyan circles) were obtained using the dual laser plasma technique (DLP) taken at a photon energy resolution of 35 meV FWHM compared with results obtained from the 456-level DARC calculations. The $\text{Rb}^+ 4s^2 4p^5 ({}^2P_{1/2}^o) nd {}^1P^o_1$ (inverted solid black triangles) are identified in the spectra. Table 3 give a comparison of the DARC resonance results with the DLP experimental and other theoretical results. The DARC photoionization cross sections (solid red line) have been convoluted with a Gaussian distribution having a 35 meV FWHM profile and an appropriate admixture used (see text for details) for the ground state and the metastable states.

ground state and 2% of the statistical average of the $4s^2 4p^5 5s {}^3P^o_{2,1,0}$, $4s^2 4p^5 5s {}^1P^o_1$, and $4s^2 4p^5 4d {}^3P^o_{2,1,0}$ metastable states.

4 CONCLUSIONS

Theoretical results from large-scale DARC photoionization cross section calculations were used to interpret the experimental data from the DLP and ASTRID facilities. From our DARC results, a resonance analysis of both the Feshbach and the Fano window resonances illustrate excellent agreement with the available experimental data. The present theoretical work may be incorporated into astrophysical modelling codes like CLOUDY (Ferland et al. 1998; Ferland 2003), XSTAR (Kallman 2001) and AtomDB (Foster et al. 2012) used

to numerically simulate the thermal and ionization structure of ionized astrophysical nebulae.

ACKNOWLEDGEMENTS

BMMcL acknowledges support by the US National Science Foundation through a grant to ITAMP at the Harvard-Smithsonian Center for Astrophysics under the visitors program, the University of Georgia at Athens for the award of an adjunct professorship, and Queen's University Belfast for the award of a visiting research fellowship (VRF). ITAMP is supported in part by NSF Grant No. PHY-1607396. The hospitality of Professor Thomas J Morgan and Wesleyan University, Middletown, CT, USA are gratefully acknowledged, where this research was completed. We thank Captain Thomas J Lavery USN Ret. for his constructive comments which enhanced the quality of this manuscript. Professor John Costello and Dr Deirdre Kilbane, are thanked

Table 3. Resonance energies E_n of the $4s^2 4p^5 ({}^2P^{\circ}_{1/2}) nd {}^1P^{\circ}_1$ Rydberg series from the experimental measurements and the theoretical calculations (HXR approximation, Cowan code) of [Kilbane et al. \(2007\)](#) with the present 456-level DARC calculations, converging to the $Rb^{2+}(3d^{10} 4s^2 4p^5 {}^2P^{\circ}_{1/2})$ threshold. The Feshbach resonances in the photoionization cross section originate out of the $4p$ -subshell from the $Rb^+(3d^{10} 4s^2 4p^6 {}^1S_0)$ ion in its ground state. The quantum defect μ for the Rydberg series and the autoionization linewidths Γ (meV) are included for completeness.

Experimental and theoretical autoionizing Rb II resonance energies, quantum defects and linewidths							
Label nd	Theory ^a E_n (eV)	Expt ^b E_n (eV)	Theory ^c E_n (eV)	Theory ^a μ_n	Expt ^b μ_n	Theory ^c μ_n	Theory ^a Γ (meV)
7d	–	–	–	–	–	–	–
8d	27.3008	27.30	27.3099	0.2376	0.1977	0.1982	32.4
9d	27.4805	27.50	27.4595	0.3265	0.2077	0.3922	17.2
10d	27.6223	27.63	27.5900	0.3257	0.2628	0.5853	12.3
11d	27.7263	27.74	27.6814	0.3253	0.1699	0.7952	9.1
12d	27.8046	27.82	27.7519	0.3246	0.0951	1.0283	6.9
13d	27.8652	27.89	27.8072	0.3243	-0.1651	1.2887	5.4
14d	27.9129	27.95	27.8515	0.3241	-0.6377	1.5746	4.3
15d	27.9512	–	–	0.3239	–	–	3.4
16d	27.9824	–	–	0.3239	–	–	2.8
⋮							
Limit	28.204	28.204	28.204	–	–	–	–

^aTheory, DARC 456-level Dirac R -matrix approximation.

^bExperiment, synchrotron radiation (SR) and dual laser plasma (DLP) ([Kilbane et al. 2007](#)).

^cTheory, Hartree-Fock with exchange plus relativistic corrections (HXR) approximation, Cowan code ([Kilbane et al. 2007](#)).

Table 4. $Rb^+ 4s \rightarrow np$ Fano window Rydberg resonance parameters for the first few members of the $4s 4p^6 ({}^2S_{1/2}) np {}^1P^{\circ}_1$ series from the present 456-level DARC calculations, and experiment, converging to the $Rb^{2+}(3d^{10} 4s 4p^6 {}^2S_{1/2})$ threshold. Theoretical results obtained from the DARC 456-level approximation are compared with previous experimental values from the ASTRID synchrotron radiation (SR) facility and the dual laser plasma (DLP) technique. The Rydberg resonance energy positions E_r are in eV and the autoionization resonances linewidths Γ are in meV.

Label np	Experiment E_r (eV)	Theory E_r (eV)	Experiment Γ (meV)	Theory Γ (meV)
5p	35.710 ± 0.02^a 35.708 ^b 35.714 ^c	35.720 ^d	90 ± 30^a 117 ^b 143 ^c	137 ^d
6p	39.442 ^b 39.436 ^c	39.448 ^d	–	38 ^d
7p	–	40.942 ^d	–	17 ^d

^aDual Laser Plasma (DLP), ([Neogi et al. 2003](#)).

^bDual Laser Plasma (DLP) and Synchrotron Radiation (SR) ([Kilbane et al. 2007](#)).

^cDual Laser Plasma (DLP), ([Neogi et al. 2003](#)) corrected by [Kilbane et al. \(2007\)](#).

^dDARC, 456-level approximation, present work.

for the provision of the ASTRID and DLP data in numerical format. The authors acknowledge this research used grants of computing time at the National Energy Research

Scientific Computing Centre (NERSC), which is supported by the Office of Science of the U.S. Department of Energy (DOE) under Contract No. DE-AC02-05CH11231. The authors gratefully acknowledge the Gauss Centre for Supercomputing e.V. (www.gauss-centre.eu) for funding this project by providing computing time on the GCS Supercomputer HAZEL HEN at Höchstleistungsrechenzentrum Stuttgart (www.hlr.de). ITAMP is supported in part by NSF Grant No. PHY-1607396.

REFERENCES

- Ballance C. P., Berrington K. A., McLaughlin B. M., 1999, *Phys. Rev. A*, **60**, R4217
- Berkowitz J., 1979, *Photoabsorption, Photoionization and Photoelectron Spectroscopy*. Academic Press, New York, USA
- Darling J., 2018, *Research Notes of the AAS*, **2**, 15
- Demekhin P. V., et al., 2007, *Optics and Spectroscopy*, **102**, 149
- Dyall K. G., Johnson C. T., Grant I. P., Parpia F., Plummer E. P., 1989, *Comput. Phys. Commun.*, **55**, 425
- Fano U., Cooper J. W., 1968, *Rev. Mod. Phys.*, **40**, 441
- Ferland G. J., 2003, *Ann. Rev. of Astron. Astrophys.*, **41**, 517
- Ferland G. J., Korista K. T., Verner D. A., Ferguson J. W., Kingdon J. B., Verner E. M., 1998, *Pub. Astron. Soc. Pac. (PASP)*, **110**, 761
- Foster A. R., Ji L., Smith R. K., Brickhouse N. S., 2012, *Astrophys. J.*, **756**, 128
- Frebel A., Simon J. D., Kirby E. N., 2014, *ApJ*, **786**, 74
- Grant I. P., 2007, *Quantum Theory of Atoms and Molecules: Theory and Computation*. Springer, New York, USA
- Hinojosa G., et al., 2017, *MNRAS*, **470**, 4048
- Kallman T. R., 2001, *Astrophys. J. Suppl. Ser.*, **134**, 139
- Kilbane D., et al., 2007, *Phys. Rev. A*, **75**, 032711
- Kramida A. E., Ralchenko Y., Reader, J. and NIST ASD Team 2018, *NIST Atomic Spectra Database* (version 5.5.2), Na-

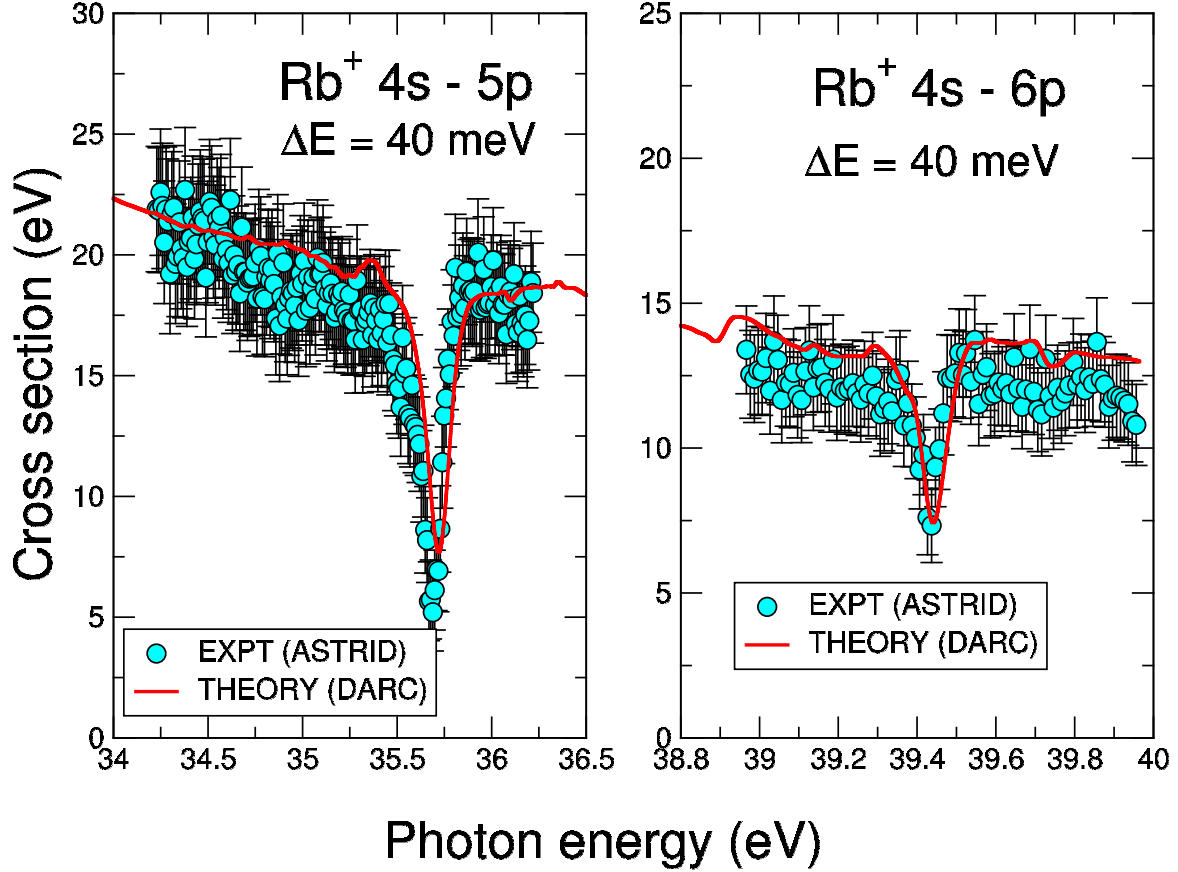


Figure 4. (Colour online) Single photoionization cross section of Rb^+ in the photon energy regions of the two major Fano window resonances, respectively, 34 – 36.5 eV and 38.8 – 40 eV. Experimental measurements (solid cyan circles) were obtained from the ASTRID radiation facility, in Aarhus, Denmark, at a photon energy resolution of 40 meV FWHM, compared with results obtained from the 456-level (DARC) approximation. The DARC photoionization cross sections (solid red line) have been convoluted with a Gaussian distribution having a 40 meV FWHM profile and an appropriate admixture used (see text for details) for the ground and the metastable states.

tional Institute of Standards, Technology, Gaithersburg, MD, USA, <http://physics.nist.gov/>

Mishenina T. V., Kovtyukh V. V., Soubiran C., Travaglio C., Busso M., 2002, *A&A*, **396**, 189

Mueller A., et al., 2013, *Bull. Am. Phys. Soc.*, **58**, Q1.00141

Müller A., et al., 2017, *J. Phys. B: At. Mol. Opt. Phys.*, **50**, 205001

Neogi A., et al., 2003, *Phys. Rev. A*, **67**, 042707

Parpia F., Froese-Fisher C., Grant I. P., 2006, *Comput. Phys. Commun.*, **94**, 249

Quigley L., Berrington K. A., 1996, *J. Phys. B: At. Mol. Opt. Phys.*, **29**, 4529

Quigley L., Berrington K. A., Pelan J., 1998, *Comput. Phys. Commun.*, **114**, 225

Roederer I. U., Sneden C., Thompson I. B., Preston G. W., Shectman S. A., 2010, *ApJ*, **711**, 573

Roederer I. U., Marino A. F., Sneden C., 2011, *ApJ*, **742**, 37

Shore B. W., 1967, *Rev. Mod. Phys.*, **39**, 439

Smith F. T., 1960, *Phys. Rev.*, **118**, 349

Sneden C., Gratton R. G., Crocker D. A., 1991, *A&A*, **246**, 354

This paper has been typeset from a $\text{\TeX}/\text{\LaTeX}$ file prepared by the authors.